

## Immunogenicity of inactivated rotavirus in rhesus monkey, and assessment of immunologic mechanisms

Yan Zhou, Jinyuan Wu, Xiaoqing Hu, Rong Chen, Xiaochen Lin, Na Yin, Chenxing Lu, Jun Ye, Yongmei Zhao, Xiaopeng Song, Zexin Song, Jinlan Wang, Yan Li, Jinmei Li, Guangming Zhang, Maosheng Sun & Hongjun Li

**To cite this article:** Yan Zhou, Jinyuan Wu, Xiaoqing Hu, Rong Chen, Xiaochen Lin, Na Yin, Chenxing Lu, Jun Ye, Yongmei Zhao, Xiaopeng Song, Zexin Song, Jinlan Wang, Yan Li, Jinmei Li, Guangming Zhang, Maosheng Sun & Hongjun Li (2023) Immunogenicity of inactivated rotavirus in rhesus monkey, and assessment of immunologic mechanisms, Human Vaccines & Immunotherapeutics, 19:1, 2189598, DOI: [10.1080/21645515.2023.2189598](https://doi.org/10.1080/21645515.2023.2189598)

**To link to this article:** <https://doi.org/10.1080/21645515.2023.2189598>



© 2023 The Author(s). Published with license by Taylor & Francis Group, LLC.



[View supplementary material](#)



Published online: 30 Mar 2023.



[Submit your article to this journal](#)



Article views: 1949



[View related articles](#)



[View Crossmark data](#)



Citing articles: 5 [View citing articles](#)

RESEARCH ARTICLE

OPEN ACCESS



## Immunogenicity of inactivated rotavirus in rhesus monkey, and assessment of immunologic mechanisms

Yan Zhou\*, Jinyuan Wu\*, Xiaoqing Hu, Rong Chen, Xiaochen Lin, Na Yin, Chenxing Lu, Jun Ye, Yongmei Zhao, Xiaopeng Song, Zexin Song, Jinlan Wang, Yan Li, Jinmei Li, Guangming Zhang, Maosheng Sun, and Hongjun Li 

Institute of Medical Biology, Chinese Academy of Medical Science & Peking Union Medical College, Yunnan Key Laboratory of Vaccine Research and Development on severe Infectious Disease, Kunming, China

### ABSTRACT

Rotavirus is one of the main pathogens causing severe diarrhea in infants and young children < 5 years of age. The development of the next-generation rotavirus vaccine is of great significance for preventing rotavirus infection and reducing severe mortality. The current study aimed to develop and evaluate the immunogenicity of inactivated rotavirus vaccine (IRV) in rhesus monkeys. Monkeys received two or three IRV injections intramuscularly at a 4-week interval. Neutralizing antibodies, cellular immunity, PBMC gene expression profiling, and immune persistence were evaluated. Three-dose immunization of IRV induced a higher level of neutralizing, IgG and IgA antibodies compared to two-dose immunization. IRV induced IFN- $\gamma$  secretion to mediate cellular immune responses, including robust pro-inflammatory and antiviral responses. Chemokine-mediated signaling pathways and immune response were broadly activated by IRV injection. The IRV-induced neutralizing antibodies resulting from two doses returned to baseline levels 20 weeks after full immunization, while those resulting from three doses returned to baseline levels 44 weeks after full immunization. Increasing immunization dose and injection number will help to improve IRV immunogenicity and neutralizing antibody persistence.

### ARTICLE HISTORY

Received 6 October 2022  
Revised 6 February 2023  
Accepted 20 February 2023

### KEYWORDS

Rotavirus; inactivated rotavirus vaccine; immunogenicity; immunologic mechanism; rhesus monkey

## Introduction

Rotavirus, a double-stranded non-enveloped RNA virus, is one of the main pathogens causing severe diarrhea in infants and young children < 5 years of age.<sup>1–5</sup> Rotavirus caused an estimated > 500,000 childhood deaths and > 2 million hospitalizations worldwide in 2000.<sup>4</sup> In 2013, rotavirus infections alone led to approximately 215,000 deaths in children under 5 years old worldwide.<sup>5–7</sup> Presently, there is no effective specific treatment available for patients with rotavirus infections. Vaccination is an effective strategy to prevent and control rotavirus infection and reduce severe mortality. Since live rotavirus vaccines became available in 2006, the number of child deaths due to rotavirus disease decreased from 77% to 59%.<sup>3,5,8,9</sup> Six live rotavirus vaccines are currently in use, including Rotarix (G1P[8]; GlaxoSmithKline Biologicals, Rixensart, Belgium), RotaTeq (G1P[5], G2P[5], G3P[5], G4P [5], G6P[8]; Merck & Co. Inc., Whitehouse Station, NJ, USA), Rotavac (G9P[11]; Bharat Biotech International Ltd., India), ROTASIIL(G1P[5],G2P[5],G3P[5],G4P[5]and G9P[5]; Serum Institute of India, India), Lanzhou lamb rotavirus vaccine (G10P[15]; Lanzhou Institute of Biomedical Products, Lanzhou, China) and Rotavin-M1(G1P[8]; Polyvac, Vietnam,)[5].<sup>7–13</sup> Live rotavirus vaccines have had a significant impact on reducing the rotavirus disease burden.

However, their effectiveness is blunted in resource-limited settings compared to in high- and middle-income countries.<sup>14–17</sup> The reasons for the observed discrepancy in the performance of oral rotavirus vaccines include environmental enteropathy, malnutrition, the intestinal microbiome and virome, and high levels of transplacental maternal antibodies.<sup>15,18,19</sup> The development of various forms of vaccines, including inactivated rotavirus vaccines<sup>20–22</sup> and genetically engineered vaccines,<sup>23–25</sup> is a necessary supplement to live attenuated rotavirus vaccines and is also actively explored for vaccine improvement. In the case of inactivated vaccines, Jiang et al. have been studying inactivated vaccines for many years.<sup>20–28</sup> Their results demonstrated that a candidate inactivated vaccine named CDC IRV9, human strain CDC-9 (G1P [8]) formulated with aluminum phosphate, fights rotavirus infection in gnotobiotic piglets.<sup>26</sup> IRV9 can induce broad cross-protective immunity against human rotavirus strains.<sup>29</sup> In the case of genetically engineered vaccines, rotavirus sub-unit vaccine P2-VP8 developed by the NIH is already in the clinical trial phase. The Phase I clinical trial and Phase I/II clinical trials were conducted in Baltimore<sup>30</sup> and South Africa, respectively.<sup>24</sup> The vaccine was well tolerated, and vaccinated infants demonstrated strong IgG responses (>98% seroconversion) compared with the placebo (9% seroconversion).

**CONTACT** Hongjun Li   [lihj6912@163.com](mailto:lihj6912@163.com) Institute of Medical Biology, Chinese Academy of Medical Science & Peking Union Medical College, No. 935, Jiaolong Road, Kunming, Yunnan 650118, China.

\*These authors contributed equally to this work.

 Supplemental data for this article can be accessed on the publisher's website at <https://doi.org/10.1080/21645515.2023.2189598>

© 2023 The Author(s). Published with license by Taylor & Francis Group, LLC.

This is an Open Access article distributed under the terms of the Creative Commons Attribution-NonCommercial-NoDerivatives License (<http://creativecommons.org/licenses/by-nc-nd/4.0/>), which permits non-commercial re-use, distribution, and reproduction in any medium, provided the original work is properly cited, and is not altered, transformed, or built upon in any way. The terms on which this article has been published allow the posting of the Accepted Manuscript in a repository by the author(s) or with their consent.

A trivalent subunit vaccine (P2-VP8-P[4]P[6]P[8]), which was studied using a similar design, also completed the Phase I/II clinical trial in 2020.<sup>25</sup> Strong IgG responses were demonstrated, and a neutralizing antibody response to several strains of rotavirus was also detected.

Our work focused on developing an inactivated Rotavirus vaccine (IRV), which has taken 10 years. A human wild-type rotavirus named ZTR-68-A (G1P[8]) was isolated from a child's stool with diarrhea in Zhaotong, Yunnan, China, and adapted to growth in Vero cells to prepare inactivated rotavirus vaccine. IRV is a whole virus particle-inactivated vaccine and is a second-generation rotavirus vaccine developed using traditional methods. IRV is considered safe because the virus particles are inactivated and cannot replicate in the human body. At present, there is no licensed inactivated rotavirus vaccine available worldwide.

In a previous study, mice were found to produce neutralizing anti-rotavirus antibodies following immunization with inactivated rotavirus vaccine.<sup>31</sup> To evaluate the immune response to IRV in non-human primates, 5-month-old rhesus monkeys were selected for immunogenicity studies of three IRV doses (160 ELISA units (EU), 320 EU, and 640 EU) and different immunization schedules (2 or 3 doses). The titers of neutralization, IgG and IgA antibodies in serum were determined to evaluate the immune effect of IRV. Although many vaccines can be used to prevent infectious diseases, the specific immune mechanism of vaccines is still unclear. To explore the immune mechanism of the inactivated rotavirus vaccine, PBMCs from the peripheral blood of rhesus monkeys after vaccination were collected for gene profiling detection and analyses. Humoral immunity, cellular immunity, and gene expression profiling results of monkeys are beneficial to further understanding the immune mechanism of IRV in non-human primates and will provide data for IRV clinical trials in the future.

## Materials and methods

### Cells, viruses, and vaccine

The virus named ZTR-68-A (G1P[8]) was obtained from a child with diarrhea in Yunnan province, China. Stool samples were resuspended with phosphate buffered saline (PBS) and centrifuged at a low g number, and the supernatant was inoculated into MA104 cells for adaptive culture. After 18 serial passages, further adaptive culture was conducted for 16 passages on Vero cells. ZTR-68-A (G1P[8]) is preserved by the Molecular Biology Laboratory, Institute of Medical Biology, Chinese Academy of Medical Sciences. IRV was formulated as 1280, 640, and 320 EU/mL and stored at 2–4°C until use; each 0.5-mL aliquot contained 640, 320, and 160 EU inactivated rotavirus antigen.

### Vaccine preparation

When Vero cells reached 100% confluence in a spin bottle, they were infected with the ZTR-68 strain at an MOI of 0.1 in serum-free MEM medium (Gibco, Grand Island, NY, USA). The culture media were harvested when the cytopathic effect

was complete. The infectivity of the harvested virus solution was determined using Rotavirus antigen detection kit (colloidal gold method) (WANTAI Biopharm, Beijing, China).<sup>32</sup> Cell culture media from infected cells were filtered to remove cell debris, and clarified supernatants were concentrated through ultrafiltration membrane cassettes (Sigma-Aldrich, MO, USA). Concentrated live rotaviruses were purified further by ion exchange chromatography and gel filtration (General Electric Company, USA) purification. Subsequently, the filtrates were sterilized using a 0.22-μm strainer, followed by inactivation by formaldehyde at a final concentration of 150 μg/mL for 6 days at 37°C. Upon completion of inactivation, completeness of inactivation was detected by MA104 cell passage and immunofluorescence. After HPLC detection, inactivated rotavirus of >98% purity was used for vaccine preparation. Next, the inactivated rotavirus stock solution was absorbed using Al (OH)3 adjuvant (IMBCAMS, China) to generate a semi-finished vaccine product. IRV was formulated as 1280, 640, and 320 EU/mL and stored at 2–4°C until use; each 0.5-mL aliquot contained 640, 320, and 160 EU inactivated rotavirus antigen. The amount of 640 EU corresponded to 10<sup>6</sup> virus particles.

### Vaccination procedure

Twenty-four rhesus monkeys (5 months old) were obtained from the Primate Centre of the Institute of Medical Biology, Chinese Academy of Medical Sciences. According to the immunization program, the rhesus monkeys were divided into a two-dose immunization group and a three-dose immunization group. Each of the two groups was further divided into four groups: adjuvant control (0 EU), 160 EU, 320 EU, and 640 EU. Three rhesus monkeys per group were housed in a monkey cage, and all monkeys were kept in the same room. The peripheral blood of monkeys was collected for antibody detection before immunization. Monkeys were negative for rotavirus antibody before immunization. The rhesus monkeys were vaccinated with inactivated rotavirus vaccine on the second day after blood collection by intramuscular injection. Monkeys in the two-dose immunization group were immunized twice at weeks 0 and 4 (160 EU/320 EU/640 EU each time). Monkeys in the three-dose immunization group were immunized three times at weeks 0, 4 and 8 (160 EU/320 EU/640 EU each time). In the two-dose immunization group, the sera were collected at weeks 4 and 6 to evaluate immunogenicity of the vaccine. In the three-dose immunization group, the sera were collected at weeks 4, 6, and 10 to evaluate the immunogenicity of the vaccine. In the two-dose immunization group, the sera at weeks 2, 6, 8, 12, 16, 24 and 28 were collected to evaluate the persistence of immunity. In the three-dose immunization group, the sera at weeks 2, 6, 10, 12, 28, and 52 were collected to evaluate the persistence of immunity (Figure 1).

### Detection of serum neutralization antibodies

A combined cell culture enzyme-linked immunosorbent assay (ELISA) was used to measure the levels of neutralizing antibodies in sera.<sup>33</sup> Briefly, MA104 cells were counted, seeded into 96-well microplates at a density of 20,000 cells per well,

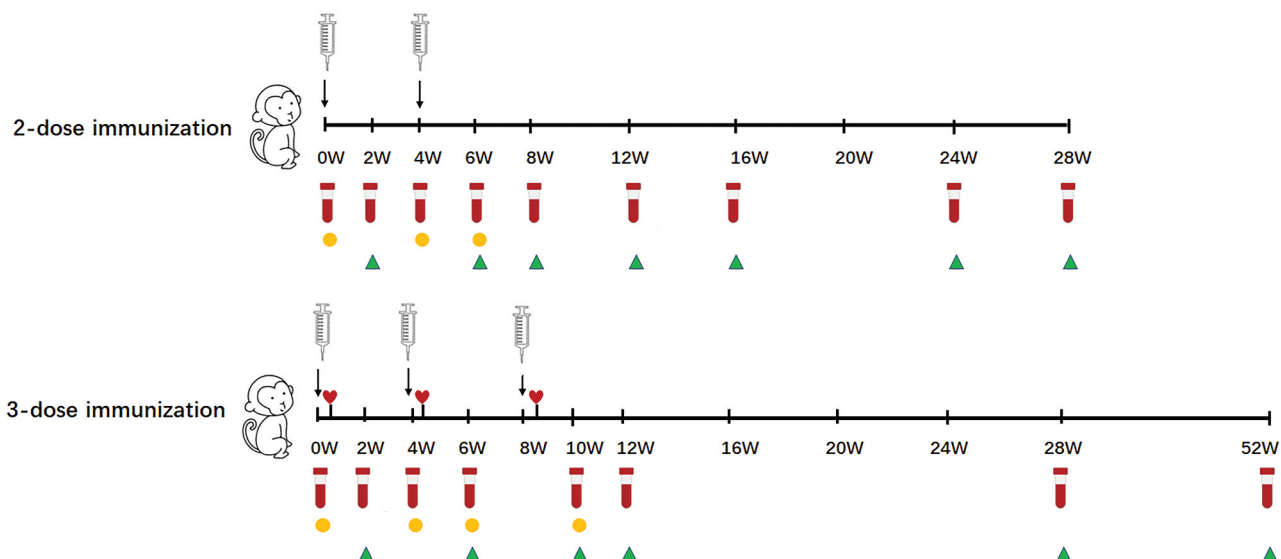


**Figure 1.** Schedule of IRV immunization and blood collection. Monkeys were immunized with different dose (160 EU, 320 EU and 640 EU) of IRV at weeks 0, 4 or 0, 4, and 8. Serum was collected from the two-dose immunization group was collected at weeks 4 and 6 for the determination of neutralizing antibodies and IgG and IgA antibodies. Serum was collected from the three-dose immunization group at weeks 4, 6 and 10 for the determination of neutralizing antibodies and IgG and IgA antibodies. Serum was collected at weeks 2, 6, 8, 12, 16, 24, and 28 in the two-dose immunization group and at weeks 2, 6, 10, 12, 28, and 52 for in the three-dose immunization group for immune persistence evaluation. The peripheral blood of monkeys 2 weeks after the whole immunization was collected to separate peripheral blood lymphocytes for IFN- $\gamma$  ELISpot detection. The peripheral blood of the monkeys was collected for cytokine detection. PBMC samples from the peripheral blood of monkeys 5 days after each dose of immunization were collected for gene profile analysis. Red tubes and red hearts represent all blood collection time points. Specifically, red hearts represent gene expression profile detection time points, yellow circles represent immunogenicity evaluation points, and green triangles represent immune persistence evaluation points.

and cultured until a confluent cell monolayer was formed. A G1 rotavirus strain previously prepared in our laboratory was used as a reference virus at a titer of 10,000 PFU (plaque forming unit)/mL. A series of two-fold serum dilutions was prepared, with an initial dilution of 1:8. Simultaneously, positive serum control wells, negative serum control wells, virus back titration wells, control cell wells, and control virus wells were prepared in at least quadruplicate. The reference virus was activated by trypsin (2.5%, GIBCO, 15090046) at a final concentration of 20  $\mu$ g/mL for 1 h at 37°C. The trypsin-activated reference rotavirus was added to wells containing serum dilutions at 100  $\mu$ L (1000 PFU) per well. The plate was incubated at 37°C for 1 h; then, the maintenance media containing MA104 cells were removed and replaced with the diluted sera, with each dilution prepared at least in duplicate. These samples were cultured at 37°C in 5% CO<sub>2</sub> incubators for 7 d and then transferred into microplates and analyzed using ELISA immunoassay at an absorbance of 450 and 650 nm (reference wavelength). When the detected value of assayed serum sample fell below the threshold, the serum sample was considered positive for rotavirus-specific neutralizing antibody; the reciprocal of this dilution ratio was designated as the serum neutralization titer value.

#### Detection of serum IgG and IgA antibodies

The microplates were coated with inactivated rotavirus overnight at 4°C. After washing, 3% bovine serum albumin (BSA) was added to the microplates for 1 h at 37°C. After washing with PBS, two-fold serial dilutions of monkey positive and negative sera were added to the microplates and incubated at 37°C for 1 h. Then, HRP-conjugated goat anti-monkey IgG antibody

(Abcam, Cambridge, UK) or HRP-conjugated goat anti-monkey IgA antibody (KPL, UK) was added to the microplates and incubated at 37°C for 1 h. Following three washes with PBS, the plates were developed with 100  $\mu$ L/well of TMB substrate (Solarbio, China) for 5 min in the dark and stopped with ELISA Stop Solution (Solarbio, China). The plates were evaluated using an EPOCH microplate reader (BioTek, USA) at an absorbance of 450 with a reference wavelength of 650 nm. If the A450 values of the serum dilution were higher than 0.105, the IgG/IgA antibody was considered to be positive, while the reciprocal of the highest positive serum dilution was considered as the IgG/IgA titer. Increasing multiple of the geometric mean titers (GMI)  $\geq 4$  was defined as the positive conversion.

#### ELISpot assay

The peripheral blood of monkeys was collected 2 weeks after the whole immunization to separate peripheral blood lymphocytes (PBMCs) for IFN- $\gamma$  ELISpot assay. Peripheral blood lymphocytes from peripheral blood were separated by monkey Lymphocyte isolates (DAKEWE, 7511011, China). IFN- $\gamma$  ELISpot detection was performed according to the instructions of the Monkey IFN- $\gamma$  ELISpot PLUS(ALP) kit (Mabtech, 3421 M-4HST-2, Sweden). The ELISpot plates were incubated with 200  $\mu$ L/well of serum-free media for 30 min at room temperature. After washing, monkey PBMCs ( $1 \times 10^5$  cells/well) and VP7 peptides (DYIIIRFLLI (31 to 40 aa), 20  $\mu$ g/mL, GenScript, Nanjing, China) were added to the ELISpot plates at 50  $\mu$ L/well. Positive stimulus (PHA+Ito) was added to the positive control wells at 1  $\mu$ L/well. The plates were incubated for 24 h at 37°C with 5% CO<sub>2</sub>. After incubation, the plates were washed five times with PBS. Biotinylated-anti-monkey IFN- $\gamma$

antibody in PBS (1:1000) was added at 100 µL/well and incubated for 1 h at room temperature. Following washing, the plates were further incubated with 100 µL/well of ALP-conjugated-Streptavidin (1:1000 dilution) for 1 h at room temperature. Following five washes with PBS, the plates were developed with 100 µL/well of BCIP/NPT-plus substrate for 5 min in the dark, before washing with water and air-drying. The immune spots in the ELISpot plates were counted using an ELISpot reader (CTL, USA) and the final spot-forming units (SFUs) were calculated as spots/million cells.

### Gene profile of PBMCs

PBMC samples of IRV immunized, and control groups were collected on day 5 after each immunization dose. Total RNAs were purified using QIAGEN RNeasy® Kit following the manufacturer's instructions. Agilent Rhesus Macaque (V2) Gene Expression (4 × 44 K; Design ID: 026806; Agilent Technologies, CA) was chosen to screen for gene expression differences in monkey PBMCs. First, microarray detection was conducted by Shanghai OE Biotech (Shanghai, China) according to the procedures described in the Agilent technical manual. Differentially expressed genes were then identified through fold change. The threshold set for upregulated and downregulated genes was a fold change  $\geq 2.0$ . Subsequently, Gene Ontology (GO) analysis and Kyoto Encyclopedia of Genes and Genomes (KEGG) analysis<sup>34</sup> were applied to determine the roles of the differentially expressed messenger RNAs (mRNAs). Next, GeneMANIA (<http://genemania.org>) was used to build a gene network according to the relationships among the genes, proteins, and compounds in the database.<sup>35,36</sup> The differential genes in specific pathways were screened and the interaction

relationship between differential genes was analyzed based on the STRING database (<https://cn.string-db.org/>). Cytoscape software was used for network visualization.

### Cytokine assay

Plasma samples from three control and three monkeys injected with 320 EU IRV were used for monkey cytokine array analyses (Cat#: QAN-CYT-1-1) of eight cytokines (RayBiotech, Norcross, GA, USA), according to the manufacturer's instructions. The fluorescent images were scanned by a microarray scanner (InnoScan 300; Innopsys, Parc d'Activites Activestre, France), and the data were analyzed with Mapix software. The cytokines were quantified according to the standard curve calibrated from the same array.

### Statistical analysis

GraphPad Prism version 8.0 (GraphPad Software, Inc. LaJolla, Calif, U.S.A.) was used for analysis and mapping. The experimental results are expressed as the geometric mean  $\pm$  the standard errors. Between-group differences were statistically analyzed using a two-tailed Student's t-test or Tukey's multiple comparison test using GraphPad Prism (Version 5.01) (GraphPad Software, San Diego, CA). *P*-values  $< 0.05$  were considered significant.

## Results

### Humoral immunoassay

To evaluate the immunogenicity of inactivated rotavirus vaccine in non-human primates, rhesus monkeys were injected with inactivated rotavirus vaccine containing 160

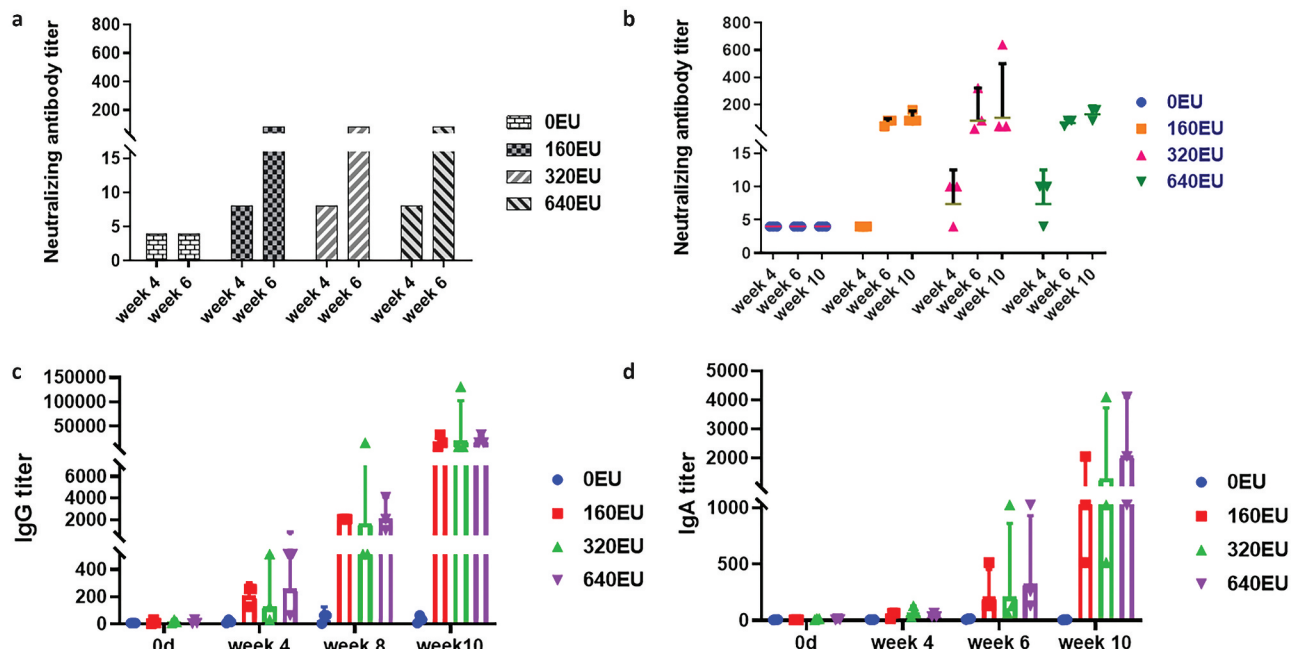


**Figure 2.** Neutralizing antibody responses after vaccine immunization. (a) Neutralizing antibodies (GMT) of monkeys at week 4 and 6 of 160 EU, 320 EU, and 640 EU in the two-dose immunization group ( $n = 3$ ). (b) Neutralizing antibodies (GMT) of monkeys at week 4, 6, and 10 of 160 EU, 320 EU, and 640 EU in the three-dose immunization group ( $n = 3$ ); (c) Anti-rotavirus IgG antibody responses in the three-dose immunization group ( $n = 3$ ). (d) Anti-rotavirus IgA antibody responses in the three-dose immunization group ( $n = 3$ ). Error bars represent the standard error of each group.

EU, 320 EU, and 640 EU via intramuscular injection (**Figure 2(a)**). Sera were collected to determine the levels of neutralizing antibodies. According to increasing multiple of the GM titers ( $GMI \geq 4$ ), the positive conversion rate of neutralizing antibodies induced by one-shot immunization was 100% for 160 EU, 320 EU, and 640 EU. In the two-dose immunization group, the neutralizing antibody titers at week 4 of 160 EU, 320 EU, and 640 EU were 8, 8, and 8, respectively, those at week 6 of 160 EU, 320 EU, and 640 EU were 80, 80, and 80, respectively (**Figure 2(a)**). In the three-dose immunization group, the neutralizing antibody titers at week 6 of 160 EU, 320 EU, and 640 EU were 63.5, 80, and 63.5, respectively (**Figure 2(b)**), while those at week 10 were 100.8, 100.8 and 126.99, respectively (**Figure 2(b)**). Here and in the following sections, all titers named are the geometrical means (GMs).

To explore whether IRV immunized rhesus monkeys can induce changes in IgG and IgA antibodies levels, sera from monkeys were collected at weeks 0, 4, 6, and 10 for the detection of IgG and IgA antibodies. According to the four-fold increase in serum IgG antibody titer, the positive conversion rates of IgG antibody induced by 160 EU, 320 EU, and 640 EU immunization were all 100%. Furthermore, the IgG antibody titer of 160 EU, 320 EU, and 640 EU were 203.19, 128 and 256 at week 4, 2048, 1625.5, and 2048 at week 6, and 16,384, 20,642.55, and 20642.55 at week 10 (**Figure 2(c)**). After two immunization doses, the IgG antibody titers increased in the 160 EU, 320 EU, and 640 EU groups were 203.17, 101.6 and 203.17, respectively (**Figure 2(c)**). After three immunization doses, the IgG antibody titers in the 160EU, 320EU, and 640EU groups were 1625.4, 1290.16 and 2047.87, respectively (**Figure 2(c)**).

According to the four-fold increase in serum IgA antibody titer, the positive conversion rate was 100%. In the three-dose immunization group, the IgA antibody titers at week 4 of 160 EU, 320 EU, and 640 EU were 40.32, 64.0 and 40.32, those at week 6 were 203.19, 203.19 and 322.54, at week 10 were 1024.0, 1290.16 and 2048.0, respectively (**Figure 2(d)**). After two immunization doses, the IgA antibody titer of the 160 EU, 320 EU, and 640 EU groups increased to 40.64, 16.0, and 40.32, respectively (**Figure 2(d)**). After three immunization doses, the IgA antibody titer of the 160 EU, 320 EU, and 640 EU groups increased to 203.17, 101.59, and 256, respectively (**Figure 2(d)**).

### Immune persistence analysis

To evaluate the immune persistence of the vaccine, in the two-dose immunization group, sera were collected at weeks 2, 6, 8, 12, 16, 24 and 28 to detect the serum neutralizing antibody (**Figure 3(a)**, **Table 1**). In the two-dose 160 EU, 320 EU and 640 EU immunization group, the sera neutralizing antibody titers at week 24 were 25.2, 31.75 and 63.5, respectively (**Figure 3(a)**, **Table 1**). In the two-dose 160 EU, 320 EU and 640 EU immunization group, the sera neutralizing antibody titers at week 28 were 6.84, 5.43 and 14.74, respectively (**Figure 3(a)**, **Table 1**). The maintenance time of neutralizing antibodies was approximately 20 weeks after two immunization doses. In the three-dose immunization group, the sera were collected at weeks 2, 6, 10, 12, 28, and 52 to evaluate the three-dose immunity persistence (**Figure 3(a)**, **Table 1**). In the three-dose 160 EU, 320 EU and 640 EU immunization group, the serum neutralizing antibody titers at week 28 were 80, 40 and 63.5, respectively (**Figure 3(b)**, **Table 1**). In the three-dose 160 EU, 320 EU and

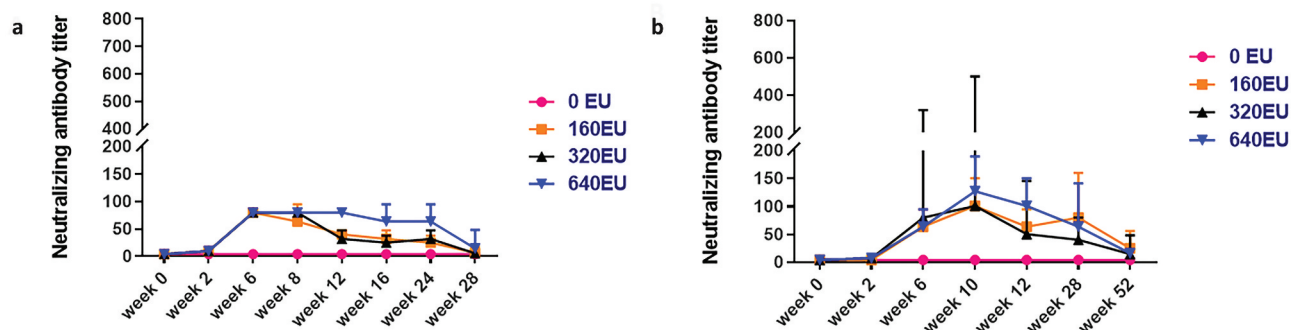


**Figure 3.** Neutralizing antibody responses in immune persistence evaluation. (a) Neutralizing antibodies (GMT) of monkeys in the two-dose immunization group at week 0, 2, 6, 8, 12, 16, 24, and 28 ( $n = 3$ ). (b) Neutralizing antibodies (GMT) of monkeys in the three-dose immunization group at weeks 2, 6, 10, 12, 28, and 52 ( $n = 3$ ).

**Table 1.** Neutralizing antibodies (GMT) of monkeys in two- and three-dose immunization group.

Week	0	2	6	8	10	12	16	24	28	52
<b>2 dose group</b>										
0EU	4	4	4	4	/	4	4	4	4	/
160EU	4	10	80	63.5	/	40	31.75	25.2	6.84	/
320EU	4	10	80	80	/	31.75	25.2	31.75	5.43	/
640EU	4	10	80	80	/	80	63.5	63.5	14.74	/
<b>3 dose group</b>										
0EU	4	4	4	/	4	4	/	/	4	4
160EU	4	4	63.5	/	100.8	63.5	/	/	80	25.2
320EU	4	7.37	80	/	100.8	50.4	/	/	40	14.74
640EU	4	7.37	63.5	/	126.99	100.79	/	/	63.5	15.87

640 EU immunization group, the serum neutralizing antibody titers at week 52 were 25.2, 14.74 and 15.87, respectively (Figure 3(b), Table 1). The maintenance time of neutralizing antibodies was approximately 44 weeks after three immunization doses.

### Cellular immunoassay

To analyze whether the inactivated rotavirus vaccine can induce a cellular immune response after immunization of rhesus monkeys, we collected the peripheral blood of rhesus monkeys 14 d after the whole immunization to separate peripheral blood lymphocytes for IFN- $\gamma$  ELISpot detection. VP7-specific IFN-gamma responses could be elicited by IRV after vaccination (Figure 4(a)). Th1 cells were activated after IRV immunization.

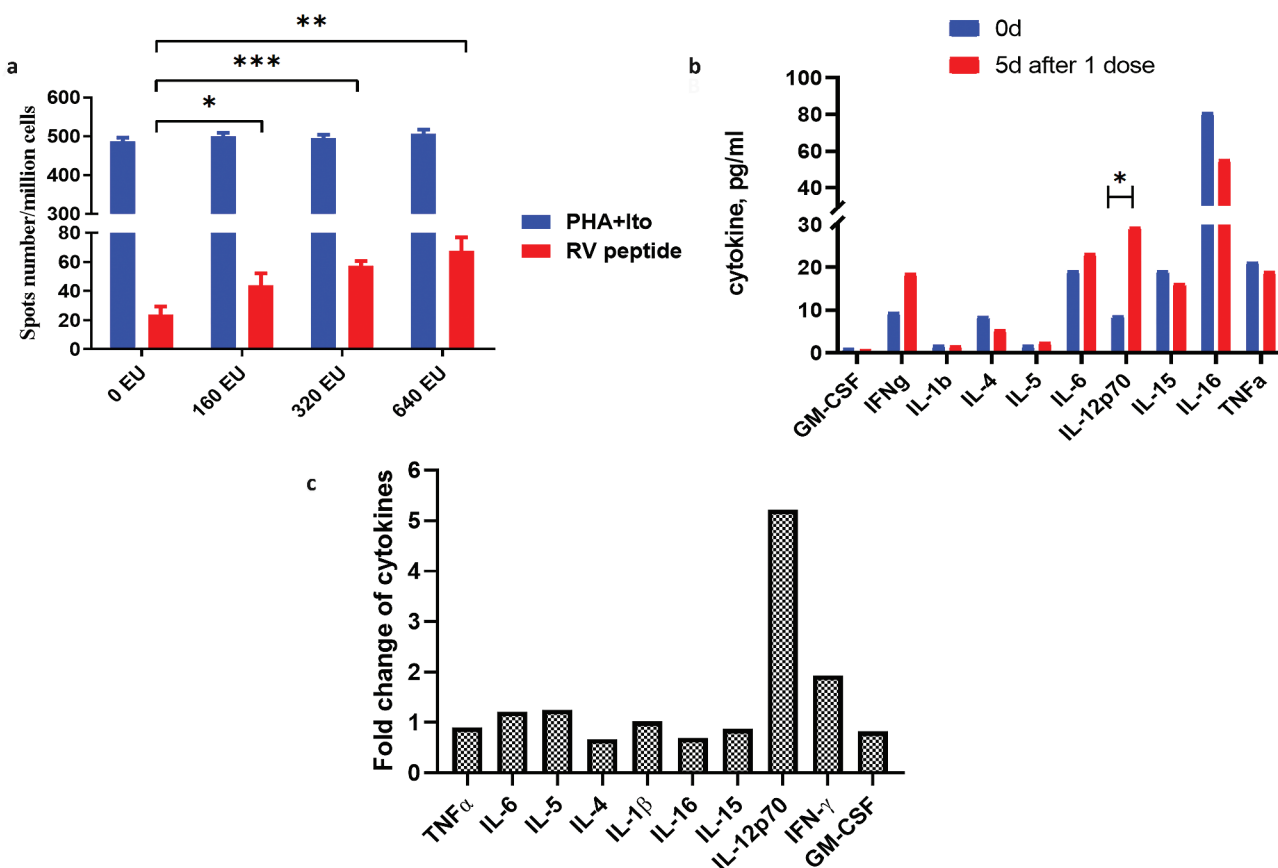
To detect the secretion of cytokines in the peripheral blood of rhesus monkeys, the peripheral blood of the rhesus monkeys in the 640 EU immunized group was collected 5 d after the first dose. Cytokines (TNF- $\alpha$ , IL-6, IL-5, IL-4, IL-1 $\beta$ , IL-16, IL-15, IL-12p70, IFN- $\gamma$ , and GM-CSF) were quantified by Quantibody® array. The results showed that, compared to blood samples before immunization, TNF $\alpha$  level in sera was downregulated by 0.67-fold, IL-6 was upregulated by 1.21-fold, IL-5 was upregulated by 1.25-fold, and IL-4 was downregulated by 0.67-fold, IL-1 $\beta$  was upregulated by 1.02-fold, IL-16 was downregulated by 0.69-fold, IL-15 was downregulated by 0.87-fold, IL-12p70 was

upregulated by 5.22-fold, IFN- $\gamma$  was upregulated by 1.93 times, and GM-CSF was downregulated by 0.82-fold (Figure 4(b,c)).

### Gene profile analysis of PBMCs

To explore the immune mechanism of the inactivated rotavirus vaccine, we collected PBMC samples from the peripheral blood of rhesus monkeys in the three-dose immunization group before immunization and 5 d after each immunization dose. Total RNA was extracted using TRIzol reagent for gene expression profiling. Differentially expressed genes were then identified through fold change. The threshold set for up-and downregulated genes was a fold change  $\geq 2.0$ . Compared to the genes before immunization, there were 479 upregulated genes and 494 downregulated genes after one dose of immunization. Among these differentially expressed genes, *PTPN21* had the highest upregulated level after one dose, and *MMP8* had the highest downregulated level (Table 2).

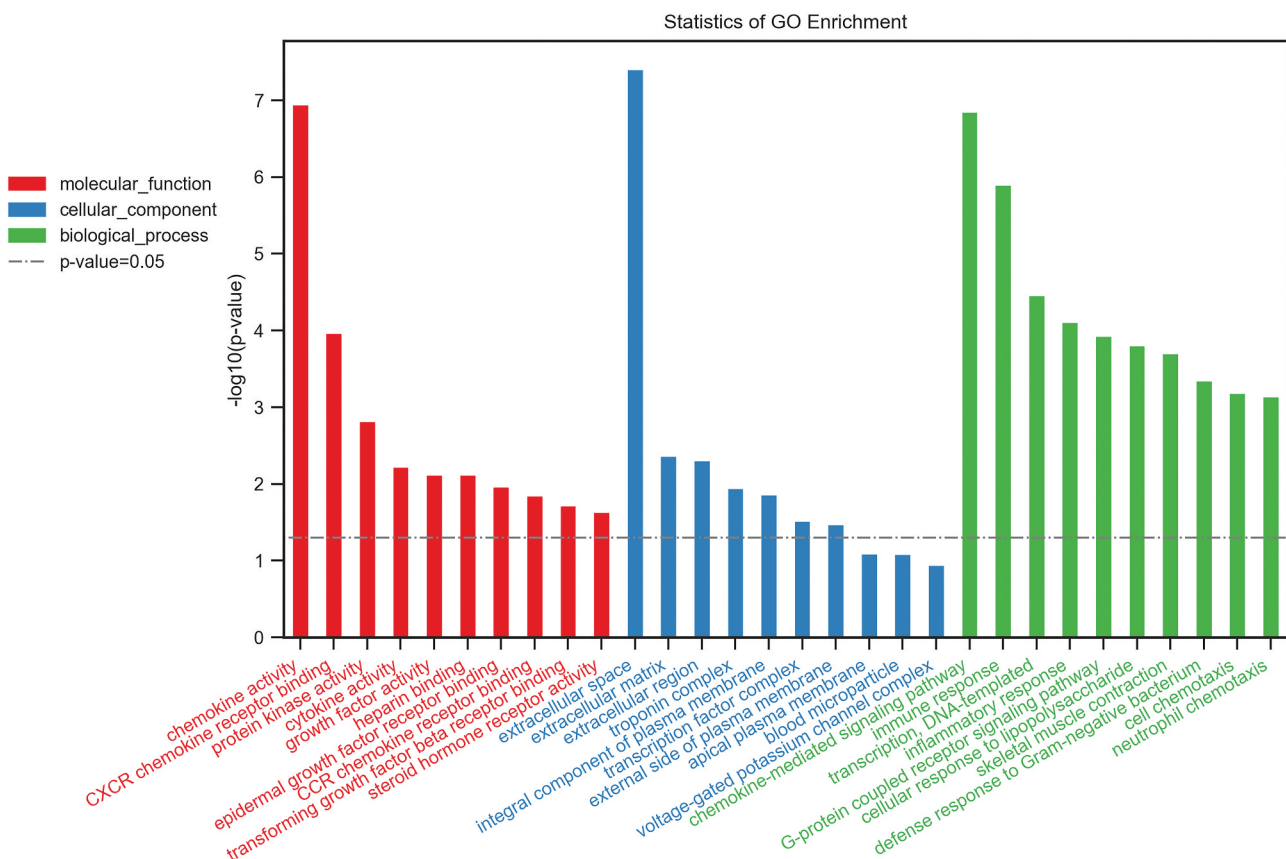
The differentially expressed genes after each immunization were subjected to GO analysis, including Biological Process, Cellular Component, and Molecular Function analysis (Figure 5). On day 5 after the first vaccine dose, the differentially expressed genes were mainly concentrated in “Chemokine -mediated signaling pathway and immune response” in Biological Process analysis; “extracellular space” in Cellular Component analysis; and “chemokine



**Figure 4.** Cellular immunoassay of monkeys after IRV vaccination conducted via IFN- $\gamma$  ELISPOT detection and cytokine array. (a) VP7-specific IFN- $\gamma$  response of monkeys on week 2 after the last vaccination. IFN- $\gamma$  ELISPOT detection was performed according to the instructions of the Monkey IFN- $\gamma$  ELISPOT PLUS(AlP) kit (MABTECH, 3421 M-4HST-2); (b) Cytokines (TNF- $\alpha$ , IL-6, IL-5, IL-4, IL-1 $\beta$ , IL-16, IL-15, IL-12p70, IFN- $\gamma$ , and GM-CSF) of plasma were quantified via Quantibody® array (\*:  $p < .05$ ; \*\*:  $p < .01$ ; \*\*\*:  $p < .001$ ); (c) Fold change of cytokines (TNF- $\alpha$ , IL-6, IL-5, IL-4, IL-1 $\beta$ , IL-16, IL-15, IL-12p70, IFN- $\gamma$ , and GM-CSF) after IRV vaccination. (\*:  $p < .05$ ).

**Table 2.** Top 10 up-regulated and down-regulated differential genes of 1 dose.

Gene symbol	FC (5d post 1 dose vs 0d)	Gene name	Regulation
MMP8	33.78832	matrix metallopeptidase 8 [Source:HGNC Symbol;Acc:HGNC:7175] [ENSMUT0000006359]	Down
NLRP5	17.72274	Macaca mulatta NLR family, pyrin domain containing 5 (NLRP5), mRNA [NM_001127631]	Down
FA2H	16.24441	Macaca mulatta fatty acid 2-hydroxylase (FA2H), mRNA [NM_001194422]	Down
KRT80	15.94529	keratin 80, type II [Source:HGNC Symbol;Acc:HGNC:27056] [ENSMUT00000046595]	Down
SLC13A1	13.85716	solute carrier family 13 (sodium/sulfate symporter), member 1 [Source:HGNC Symbol;Acc:HGNC:10916] [ENSMUT0000023562]	Down
POTEH	13.06603	Uncharacterized protein [Source:UniProtKB/TrEMBL;Acc:F6RVJ3] [ENSMUT0000044361]	Down
DDN	12.94682	dendrin [Source:HGNC Symbol;Acc:HGNC:24458] [ENSMUT0000022050]	Down
SPAG11B	12.9059	Macaca mulatta sperm associated antigen 11B (SPAG11B), transcript variant C, mRNA [NM_001110256]	Down
PAXBP1	11.15209	PAX3 and PAX7 binding protein 1 [Source:HGNC Symbol;Acc:HGNC:13579] [ENSMUT0000017222]	Down
NXPH2	10.7425	neurexophilin 2 [Source:HGNC Symbol;Acc:HGNC:8076] [ENSMUT0000007289]	Down
PTPN21	40.4079	protein tyrosine phosphatase, non-receptor type 21 [Source:HGNC Symbol;Acc:HGNC:9651] [ENSMUT0000013362]	Up
AQP4	22.15618	Macaca mulatta aquaporin 4 (AQP4), mRNA [NM_001257671]	Up
NR4A3	21.30339	nuclear receptor subfamily 4, group A, member 3 [Source:HGNC Symbol;Acc:HGNC:7982] [ENSMUT0000015979]	Up
KIAA1217	15.53657	KIAA1217 [Source:HGNC Symbol;Acc:HGNC:25428] [ENSMUT0000043132]	Up
TEK	14.33142	TEK tyrosine kinase, endothelial [Source:HGNC Symbol;Acc:HGNC:11724] [ENSMUT0000008499]	Up
AREG	13.97574	amphiregulin [Source:HGNC Symbol;Acc:HGNC:651] [ENSMUT00000003274]	Up
LAMP5	13.01566	Macaca mulatta lysosomal-associated membrane protein family, member 5 (C20orf103), mRNA [NM_001194698]	Up
NRK	12.55594	Nik related kinase [Source:HGNC Symbol;Acc:HGNC:25391] [ENSMUT0000047863]	Up
CXCL1	11.98848	growth-regulated alpha protein [Source:RefSeq peptide;Acc:NP_001028050] [ENSMUT0000042190]	Up
LOC709809	11.93836	growth-regulated alpha protein [Source:RefSeq peptide;Acc:NP_001028050] [ENSMUT0000042190]	Up

**Figure 5.** Gene Ontology (GO) analysis of differentially expressed genes between pre-immunization and 5 days after the first immunization in the three-dose immunization group. Differential genes with a fold change  $\geq 2.0$  were chosen for GO analysis, including biological process, cellular component, and molecular function analysis.

activity and CXCR chemokine receptor binding" in Molecular Function analysis (Figure 5, Table 3). On day 5, after the second vaccine dose, the differentially expressed genes were mainly concentrated in "Chemokine -mediated signaling pathway and immune response" in Biological

Process analysis; "extracellular region and extracellular space" in Cellular Component analysis; "chemokine activity" and "CXCR chemokine receptor binding" in Molecular Function analysis (Suppl. Figure S1, Table 4). On day 5, after the third vaccine dose, the differentially expressed

**Table 3.** Top 3 gene enrichment of GO analysis post 1 dose.

GO name	Genes
<b>Molecular function</b>	
chemokine activity	CXCL1, CCL3, CXCL9, CCL8, CXCL8, CXCL1, CXCL11, CXCL12, LOC100423954, CXCL10
CXCR chemokine receptor binding	CXCL1, CXCL9, CXCL8, CXCL12, CXCL10
protein kinase activity	PDIK1L, GUCY2F, CCL3, STYK1, PLK3, NEK2, MAP3K8, CCL8, NRK, MAPK7, RIPK4, CDKL5, GUCY2D
<b>Cellular component</b>	
extracellular space	CXCL1, LALBA, IBSP, CSF2, CCL3, MMP8, EDN1, CXCL9, CXCL8, CCL8, FASLG, CX3CL1, CXCL11, GREM2, IL10, CXCL10, TGFB2, ZFC3H1, SERPINE2, ALB, SERPINE1, PTH, TGFA, COL12A1, SEMA3B, THBS4, LOC698176, MDGA1, IL25, HILPDA, C4BPB, TCN1, IL22, LOC100423954, INHBB, MSMP, INHBA, ADM, DEFA4, GDF10, HBEGF, COL1A1, AREG, IL12B
extracellular matrix	IBSP, SERPINE2, SERPINE1, MMP8, COL12A1, MMP1, AHSG, TGFB2
extracellular region	FGF5, PNLLPRP1, EDN1, CXCL9, IL25, CX3CL1, PDYN, CXCL12, IL10, TGFB2, INHBB, INHBA, SPAG11B, IL1RAP, PLA2G2D, FN1, THBS4
<b>Biological process</b>	
chemokine-mediated signaling pathway	CXCL1, CCL3, CXCL9, CCL8, CXCL8, CX3CL1, CXCL11, CXCL12, LOC100423954, CXCL10
immune response transcription, DNA-templated	CXCL1, CSF2, CXCL9, CTLA4, FASLG, CXCL8, CCL8, CX3CL1, CXCL11, IL22, CXCL12, IL10, CXCL10, CD36, IL12B, NFIL3, TNFAIP3, CD28, SMAD9, TBX5, ZNF287, TBX20, E2F8, SCML1, NR4A2, FOXN1, TP53, FASLG, ESR2, NR4A3, ZSCAN4, ZKSCAN3, ID1, ZNF397, TFDP3, PIAS2, ZSCAN23, LOC696797, SIM1

**Table 4.** Top 3 gene enrichment of GO analysis post 2 dose.

GO name	Genes
<b>Molecular function</b>	
chemokine activity	CCL1, CCL23, CCL8, CXCL11, CXCL12, CCL26, CXCL10
oxygen transporter activity	HBM, HBA2, HBG2, HBB
heparin binding	BMP4, CCL23, WISP3, HBEGF, COL25A1, CXCL11, GREM2, CXCL10
<b>Cellular component</b>	
extracellular region	BMP4, PNLLPRP1, DEFB122, EDN1, DEFB128, HP, FGF22, UTS2B, CXCL12, MFRP, C1QTNF9, DKK3, ISG15, PENK, ATG4C, WISP3, SPAG11B, KLKB1, IL1RAP, PGA4, COL8A1, FN1
extracellular space	CCL1, IBSP, WNT16, MMP8, EDN1, HFE, CCL8, CXCL11, GREM2, CXCL10, CCL26, VCAM1, CCL23, KLKB1, COL6A3, TGFA, VWA2, BMP4, SPARCL1, LOC698176, PODXL, ARTN, SERPING1, COL25A1, C4BPB, PROM1, CHRD1, CPE, CPXM1, SERPINB2, GDF10, HBEGF, WNT11, AREG, IL12B, CPB2, VLDR
hemoglobin complex	HBM, HBA2, HBG2, HBB
<b>Biological process</b>	
chemokine-mediated signaling pathway	CCL1, CCL23, CCL8, CXCL11, CXCL12, CCL26, CXCL10
Positive regulation of smooth muscle cell	BMP4, HMOX1, EDN1, HBEGF, NR4A3
cell chemotaxis	CCL1, C5AR2, CCL23, HBEGF, CCL8, CXCL12

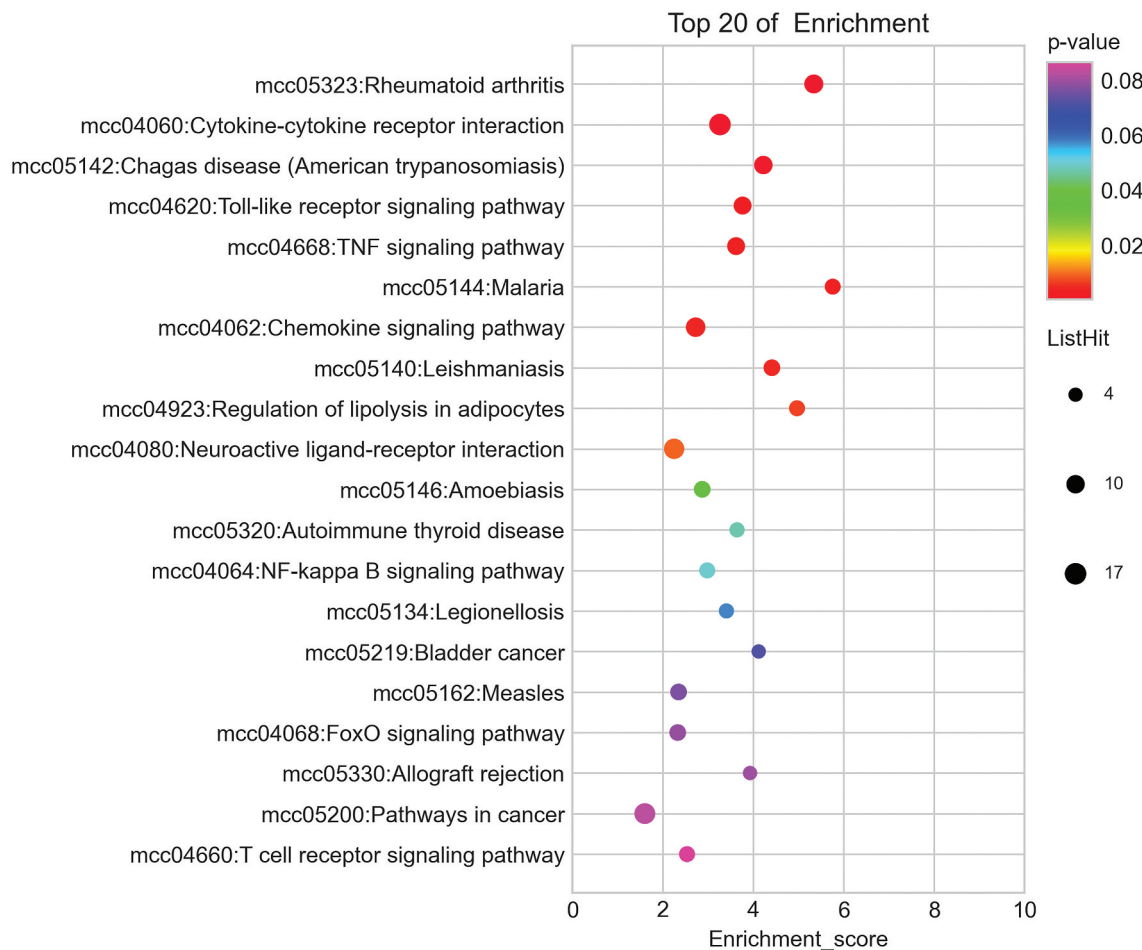
genes were mainly concentrated in the “defense response” and “Chemokine-mediated signaling pathway” in the Biological Process analysis; the “extracellular space” in the Cellular Component analysis; and the “chemokine activity” in the Molecular Function analysis (Suppl. Figure S3,

Table 5). KEGG analysis results showed that the differential genes were mainly clustered in “Cytokine-cytokine receptor interaction” (Figure 6, Suppl. Figures S2 and S4).

The differential genes in the top three GO terms were analyzed after each immunization. After the first

**Table 5.** Top 3 gene Enrichment of GO analysis post 3 dose.

GO name	Genes
<b>Molecular function</b>	
chemokine activity	CCL1, CCL23, CCL2, CXCL9, CCL8, CXCL8, CXCL11, CXCL12, CXCL10
oxygen binding	CYP2F1, ALB, HBM, HBG2, HBB
heparin binding	FGFR1, CCL23, APOE, RSP03, IMPG2, HBEGF, CXCL11, GREM2, PLA2G2D, CHRD, CXCL10
<b>Cellular component</b>	
extracellular space	A2M, GDF6, EDN1, MMP8, MNP2, CXCL11, CKB, CXCL10, WNT3, SMPDL3A, COL12A1, SEMA3B, LOC574383, LOC574382, SPO1, VWA2, WNT10B, ATP4A, LOC698176, IL25, ARTN, SERPING1, VASH1, OSM, CTSL, ADAMTS9, CHRD1, CPE, ADM, LACRT, CPXM1, DEFA4, IL12B, COL1A1, CSTA, LALBA, IBSP, CCL1, CSF2, OLFM4, IL36G, CCL2, ENPP2, CXCL9, HFE, CXCL8, CCL8, KIT, GREM2, VCAM1, CCL23, LOC574309, ALB, EPX, KLKB1, ROAD-1, RTD1A, RTD1B, RTD1C, MNP1A, ROAD2, SOST, GDF10, HBEGF, AREG, CHRD, CPB2, VLDR
external side of plasma membrane	IL6ST, PDPN, CCR1, CXCL9, HFE, AQP4, TMC1, SLC22A11, KIT, CXCL12, CXCL10, VCAM1, SCNN1G, GFRA3, CD28
troponin complex	TNNT2, TNNT3, TNNI3, TNNI1
<b>Biological process</b>	
killing of cells of other organism	RTD1A, RTD1B, CCL23, RTD1C, MNP2, MNP1A
defense response	RTD1A, LOC574309, RTD1C, SPAG11B, LOC574383, LOC574382
chemokine-mediated signaling pathway	CCL1, CCL23, CCL2, CXCL9, CCL8, CXCL8, CXCL11, CXCL12, CXCL10



**Figure 6.** KEGG analysis of differentially expressed genes between pre-immunization and 5 days after the first immunization in the three-dose immunization group. Differential genes with a fold change  $\geq 2.0$  were chosen for KEGG analysis.

**Table 6.** Fold change of differential gene ( $FC \geq 2$ ) in chemokine activity term.

Gene	CXCL1	CCL3	CXCL9	CCL8	CXCL8	CX3CL1	CXCL11	CXCL12	LOC100423954	CXCL10	CCL1	CCL23	CCL26	CCL2
1 dose	+11.99	+2.05	+2.99	-6.67	+3.57	-3.7	-2.73	-3.54	+2.3	-2.0	/	/	/	/
2 dose	/	/	/	-5.51	/	/	-7.9	/	/	-2.71	-2.39	-2.23	+5.52	/
3 dose	/	/	-2.72	-8.95	-3.73	/	-2.07	-4.53	/	-2.91	-2.42	-2.23	/	+2.1

immunization, the highest up-regulated gene in chemokine activity term was CXCL1, the highest down-regulated gene was CCL8 (Table 6). After two doses of immunization, the highest up-regulated genes in the chemokine activity term were changed to CCL26, and the highest down-regulated chemokines was CXCL11 (Table 6). After three doses of immunization, the upregulated gene in chemokine activity terms was CCL2, while CCL8 was the highest down-regulated gene after three doses (Table 6). After the first immunization dose, genes involved in immune response included CXCL1, CSF2, CXCL9, CTLA4, FASLG, CXCL8, CCL8, CX3CL1, CXCL11, IL22, CXCL12, IL10, CXCL10, CD36, IL12B, NFIL3, TNFAIP3, and CD28.

The differentially expressed genes in the chemokine-mediated signaling pathway were screened and the interaction between differentially expressed genes was analyzed based on the STRING database (<https://cn.string-db.org/>). The results of gene network analysis showed that IRV immunization stimulated various chemokines, including

CCL8, CXCL12, CXCL10, CXCL9, CCL3, CCL3L1, CXCL8, CXCL1, CX3CL1 and CXCL11. Multiple chemokines formed a tight mutual regulatory network centered on CXCL9 (Figure 7(a)). After IRV immunization, CXCL9 plays a key central regulatory role in activating the immune response by interacting with multiple chemokines. The differentially expressed genes in the immune response pathway were screened, and the interaction relationship between differential genes was analyzed based on the STRING database. Multiple immune regulatory genes were activated, including FASLG, IL22, CD28, CTLA4, CXCL10, IL10, TNFAIP2, CXCL8, CSF2, IL12B, CX3CL1, CXCL12, CXCL11, CXCL9, CXCL1, and CCL8. Activated immune-regulated genes constitute a tight regulatory network around CSF2, CXCL12, CXCL10, CXCL1, and IL-10 in the immune response (Figure 7(b)). CSF2, CXCL12, CXCL8, and CXCL10 play a key central regulatory role in the immune response via interacting with another immune-regulated genes.

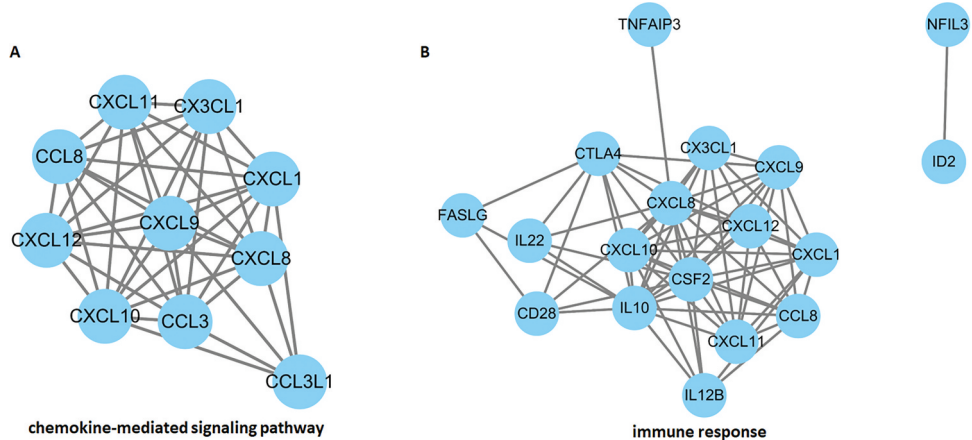


**Figure 7.** Gene network analysis. The *Chemokine-mediated signaling pathway* and *immune response* pathway were mainly activated after IRV immunization. To identify the interaction of genes in these pathways, differentially expressed genes ( $FC \geq 2$ ) in the *chemokine-mediated signaling pathway* and *immune response* term were chosen for network analysis. GeneMANIA was used to build a gene network according to the relationships among the genes. The interaction relationships of the differentially expressed genes will be represented as the gene network graphs. Each node in the graph represents one protein. The line between the nodes indicates the interaction between the two proteins. The protein with multiple connecting lines indicates the presence of multiple interactions, and the protein is the core protein. (a) Network analysis of differentially expressed genes ( $FC \geq 2$ ) in the '*chemokine-mediated signaling*' pathway; (b) Network analysis of differentially expressed genes ( $FC \geq 2$ ) in the '*immune response*'.

## Discussion

Vaccination is still the first choice for preventing severe diarrhea caused by rotavirus. The second-generation non-replicating rotavirus vaccine is a necessary complement to the live attenuated rotavirus vaccines.<sup>23,25,37</sup> Compared to live vaccines, inactivated vaccines do not cause adventitious agents contamination and reversion to virulence, especially intussusception, and can be easily combined with other vaccines, which is of great significance in eliminating rotavirus and reducing severe diarrhea mortality in infants. An IRV has also been developed by CDC for parenteral administration.<sup>20</sup> This candidate, based on a G1P[8] strain, has been tested in mice, rats, rabbits, and pig models and demonstrated a heterotypic neutralizing antibody response.<sup>26</sup> Neutralizing antibodies play an important role in challenge and protection. Systemic and mucosal immunity were shown in mice after administration via injection and via microneedle patch.<sup>20</sup> The candidate IRV (G1P[8]) presented here and the other candidate IRV (G1P[8],G9P[8]) has been tested in mice<sup>31</sup> and a rhesus monkey model<sup>22</sup> and has also induced a neutralizing antibody response. Neutralizing antibodies against rotavirus strains ZTR-68, ZTR-18, SA11, WA, UK, and Gottfried emerged in pregnant rhesus monkeys and were transplacentally transmitted to the offspring. In this study, to further explore the immunogenicity and mechanisms of IRV, humoral and cellular immunogenicity and possible mechanism of IRV were evaluated in young monkeys.

The humoral immunization results of different immunization procedures (two-dose and three-dose) showed that the serum neutralizing, IgG antibody, and IgA antibody titers were low after one dose of IRV immunization. The measurements of the three kinds of antibodies increased after the second injection. The immunization effect of the three-dose immunization group was better than that of the two-dose immunization group. Neutralizing, IgG, and IgA antibody levels were correlated with the immune dosage of IRV, especially the serum IgA antibody levels. The protective efficacy of the neutralizing, IgG

and IgA antibodies needs to be explored in future experiments with animal models and in clinical trials.

Antibody persistence is important for vaccine effectiveness. The immune persistence of IRV was evaluated by determining the neutralizing antibody levels. In the two-dose immunization group, the 640 EU group had the best immunity persistence, and the neutralizing antibody was still positive at 20 weeks after two-dose immunization. Among the three-dose immunization groups, the best immune persistence was observed in the 640 EU group. There was no significant difference between 160 EU and 320 EU. The immunization durability of the three-dose immunization group was significantly better than that of the two-dose immunization group, and the neutralizing antibodies of the three-dose groups were all positive after the three-dose immunization for 44 weeks.

To identify whether a cellular immune response could be induced after IRV injection, the peripheral blood of rhesus monkeys on day 14 after the last immunization was collected and used for IFN- $\gamma$  ELISpot detection (Figure 4). The ELISpot results indicated that IFN- $\gamma$  could be stimulated by IRV. Furthermore, eight cytokines (TNF- $\alpha$ , IL-6, IL-5, IL-4, IL-1 $\beta$ , IL-16, IL-15, IL-12p70, IFN- $\gamma$  and GM) were detected with the Quantibody® array -CSF. The expression of IL-12p70 and IFN- $\gamma$  in serum was increased, and IL-4 and IL-16 were downregulated 5 d after the first IRV immunization in rhesus monkeys. IRV immunization could stimulate the expression and secretion of IL-12, which is similar to observations made with rotavirus infection.<sup>38,39</sup> IRV immunization could also stimulate the proliferation of activated T cells, activate CD4+ T cells to differentiate into Th0 cells, promote the differentiation of Th0 cells to Th1 cells, and secrete IFN- $\gamma$ .<sup>40,41</sup> The secreted cytokines can directly fight viruses, and assist in the activation and differentiation of B cells, CD8+ T lymphocytes, and macrophages, and participate in the body's immune response. CD4+ Th1 cells are induced and mediate cellular immune responses after IRV immunization. Protection against rotavirus infection is mediated by both humoral and cellular components of the

immune system.<sup>7–46</sup> Immunogenicity induced by IRV is also mediated by both, humoral and cellular, immune responses.

To explore the immune mechanism of IRV, the total RNA of PBMC samples was extracted for gene profile assay. The immunization of rhesus monkeys with IRV can cause changes in cytokine, chemokine, and immune regulation-related genes. Chemokine-mediated signaling pathways, inflammatory response, immune response, chemokine activity, oxygen binding, and equimolecular heme-binding were activated. The main signaling pathways involved in the differential genes were cytokine-cytokine receptor interaction and chemokine signaling, which were involved in inflammation and immune response activation. On day 5, after one dose, *PTPN21*, *AQP4* and *NR4A3* showed the highest upregulation. *PTPN21* has tyrosine phosphatase activity.<sup>47</sup> *AQP4* is involved in the negative regulation of interleukin-1 beta and interleukin-6 production.<sup>48</sup> *NR4A3* also plays a role in inflammation. Upon TNF stimulation, *NR4A3* mediates monocyte adhesion by inducing the expression of *VCAM1* and *ICAM1* by binding to the NBRE consensus site.<sup>49</sup> The highest upregulated gene on day 5 after the third dose was an integrin, alpha 11, which is involved in leukocyte adhesion and transmigration of leukocytes, including T-cells and neutrophils, and is required to generate common lymphoid progenitor cells in the bone marrow.<sup>50,51</sup> Upregulated genes in chemokine activity terms included *CXCL1*, *CXCL8*, *CXCL9*, *CCL3*, and *LOC100423954*, while downregulated genes included *CCL8*, *CX3CL1*, *CXCL11*, *CXCL12*, and *CXCL10* after the first immunization. *CXCL1* has chemotactic activity for neutrophils, plays a role in inflammation, and exerts its effects on endothelial cells in an autocrine fashion.<sup>52</sup> *CXCL8* encodes interleukin-8 (IL-8), a chemotactic factor that attracts neutrophils, basophils, and T-cells, but not monocytes. It is also involved in neutrophil activation. *CXCL1* and *CXCL8* promote the development of a pro-inflammatory state along with the recruitment of other immune cells to the site of infection.<sup>53</sup> *CXCL9* encodes the C-X-C motif chemokine 9, a chemotactic factor for activated T-cells, which affects the growth, movement, or activation state of cells that participate in the immune and inflammatory response.<sup>54</sup> IRV immunization stimulated various chemokine-mediated signaling pathways. Multiple chemokines, including *CCL8*, *CXCL10*, *CXCL12*, *CCL3*, and *CXCL1*, interacted with each other and centered on *CXCL9* to promote immune responses. The gene expression profiling results further suggested that IRV releases chemokines, attracts and activates neutrophils and T-cells, and participates in immune and inflammatory responses after IRV immunization in rhesus monkeys.

In conclusion, our results demonstrated that IRV immunization could induce humoral and cellular immune responses in rhesus monkeys. Neutralizing, IgG, and IgA antibody levels were related to the immune dosage of IRV, especially the serum IgA antibody. The results of immunogenicity evaluation conducted in rhesus macaques provide reference basis for future clinical trials. The mutual regulation of immune genes, especially chemokines, further promotes immune responses. A clear immunogenic dose effect could be seen after immunization. As such, considering the presence of maternally transmitted antibodies and preexisting antibodies<sup>33</sup> in infants and

young children, three doses may be the optimal immunization dose in future clinical trials. However, due to the limited number of animals, the immunization program study was not considered. In future clinical studies, 0, 1, 2, and 0, 2, 4 immunization program studies should be further conducted and the target dose of IRV needs to be determined.

## Disclosure statement

No potential conflict of interest was reported by the author(s).

## Funding

This work was supported by the [Major Science and Technology Special Project of Yunnan Province (Biomedicine) #1] under Grant [number 202202AA100006]; [Science and Technology Project of Yunnan Province—general program #2] under Grant [number 202201AT070236]; [CAMS Innovation Fund for Medical Sciences (CIFMS) #3] under Grant [number 2021-I2M-1-043]; [Science and Technology Project of Yunnan Province—general program #4] under Grant [number 2019FB020]; and [Yunnan Province Innovative Vaccine Technology and Industrial Transformation Platform #5] under Grant [number 202002AA100009].

## ORCID

Hongjun Li  <http://orcid.org/0000-0001-5929-0071>

## Ethics statement

All animals were handled in accordance with the principles expressed in the Guide for the Care and Use of Laboratory Animals by the National Research Council of the National Academies (National Academy of Science, 2011) and The Guidance to Experimental Animal Welfare and Ethical Treatment by The Ministry of Science and Technology of the People's Republic of China. Furthermore, the Yunnan Provincial Experimental Animal Management Association (approval number: SCXK (Dian) K2017-0002) and the Experimental Animal Ethics Committee of the Institute approved the animal research (approval number: [2017]43).

## Author contributions

Yan Zhou: Conceptualization, Writing- Original draft preparation writing, Investigation, Data curation, Formal analysis. Jinyuan Wu: Methodology, Data curation, Formal analysis. Xiaoqing Hu: Investigation, Formal analysis. Rong Chen: Visualization, Data curation. Xiaochen Lin, Na Yin, Chenxing Lu, Jun Ye: Investigation. Xiaopeng Song, Jinlan Wang: Software. Yan Li, Jinmei Li: Formal analysis. Guangming Zhang: Supervision. Maosheng Sun: Supervision, Validation. Hongjun Li: Conceptualization, Writing- Reviewing and Editing.

## References

1. Crawford SE, Ramani S, Tate JE, Parashar UD, Svensson L, Hagbom M, Franco MA, Greenberg HB, O’Ryan M, Kang G, et al. Rotavirus infection. Nat Rev Dis Primers. 2017;3(1):17083. doi:[10.1038/nrdp.2017.83](https://doi.org/10.1038/nrdp.2017.83).
2. Chissaque A, Bauhofer AFL, Cossa-Moiane I, Sítio E, Munlela B, Joao ED, Langa JS, Chilaúle JJ, Boene SS, Cassocera M, et al. Rotavirus a infection in pre- and post-vaccine period: risk factors, genotypes distribution by vaccination status and age of children in Nampula Province, Northern Mozambique (2015–2019). PLoS One. 2021;16(8):e0255720. doi:[10.1371/journal.pone.0255720](https://doi.org/10.1371/journal.pone.0255720).

3. Troeger C, Khalil IA, Rao PC, Cao S, Blacker BF, Ahmed T, Armah G, Bines JE, Brewer TG, Colombara DV, et al. Rotavirus vaccination and the global burden of rotavirus diarrhea among children younger than 5 years. *JAMA Pediatr.* **2018**;172(10):958–65. doi:[10.1001/jamapediatrics.2018.1960](https://doi.org/10.1001/jamapediatrics.2018.1960).
4. Tate JE, Burton AH, Boschi-Pinto C, Steele AD, Duque J, Parashar UD. 2008 estimate of worldwide rotavirus-associated mortality in children younger than 5 years before the introduction of universal rotavirus vaccination programmes: a systematic review and meta-analysis. *Lancet Infect Dis.* **2012**;12(2):136–41. doi:[10.1016/S1473-3099\(11\)70253-5](https://doi.org/10.1016/S1473-3099(11)70253-5).
5. Tate JE, Burton AH, Boschi-Pinto C, Parashar UD. Global, regional, and national estimates of rotavirus mortality in children <5 years of age, 2000–2013. *Clin Infect Dis.* **2016**;62(suppl 2):S96–105. doi:[10.1093/cid/civ1013](https://doi.org/10.1093/cid/civ1013).
6. Li J, Wang H, Li D, Zhang Q, Liu N. Infection status and circulating strains of rotaviruses in Chinese children younger than 5-years old from 2011 to 2018: systematic review and meta-analysis. *Hum Vaccin Immunother.* **2021**;17:1811–17. doi:[10.1080/21645515.2020.1849519](https://doi.org/10.1080/21645515.2020.1849519).
7. Organization. WH. Rotavirus vaccines WHO position paper – July 2021. *Wkly Epidemiol Record.* **2021**;96:20.
8. Clark A, Black R, Tate J, Roose A, Kotloff K, Lam D, Blackwelder W, Parashar U, Lanata C, Kang G, et al. Estimating global, regional and national rotavirus deaths in children aged <5 years: current approaches, new analyses and proposed improvements. *PLoS One.* **2017**;12(9):e0183392. doi:[10.1371/journal.pone.0183392](https://doi.org/10.1371/journal.pone.0183392).
9. Collaborators GBDCoD, Abate D, Abate KH, Abay SM, Abbafati C, Abbasi N, Abbastabar H, Abd-Allah F, Abdela J, Abdelalim A, et al. Global, regional, and national age-sex-specific mortality for 282 causes of death in 195 countries and territories, 1980–2017: a systematic analysis for the global burden of disease study 2017. *Lancet.* **2018**;392(10159):1736–88. doi:[10.1016/S0140-6736\(18\)32203-7](https://doi.org/10.1016/S0140-6736(18)32203-7).
10. Burke RM, Tate JE, Kirkwood CD, Steele AD, Parashar UD. Current and new rotavirus vaccines. *Curr Opin Infect Dis.* **2019**;32(5):435–44. doi:[10.1097/QCO.0000000000000572](https://doi.org/10.1097/QCO.0000000000000572).
11. Abou-Nader A, Sauer M, Steele AD, Tate JE, Atherly D, Parashar UD, Santosham M, Nelson EAS. Global rotavirus vaccine introductions and coverage: 2006–2016. *Hum Vaccin Immunother.* **2018**;14(9):1–40. doi:[10.1080/21645515.2018.1470725](https://doi.org/10.1080/21645515.2018.1470725).
12. Soares-Weiser K, Bergman H, Henschke N, Pitan F, Cunliffe N. Vaccines for preventing rotavirus diarrhoea: vaccines in use. *Cochrane Database Syst Rev.* **2019**;2019. doi:[10.1002/14651858.CD008521.pub5](https://doi.org/10.1002/14651858.CD008521.pub5).
13. Bergman H, Henschke N, Hungerford D, Pitan F, Ndwandwe D, Cunliffe N, Soares-Weiser K. Vaccines for preventing rotavirus diarrhoea: vaccines in use. *Cochrane Database Syst Rev.* **2021**;2021(11):CD008521. doi:[10.1002/14651858.CD008521.pub6](https://doi.org/10.1002/14651858.CD008521.pub6).
14. Otero CE, Langel SN, Blasi M, Permar SR. Maternal antibody interference contributes to reduced rotavirus vaccine efficacy in developing countries. *PLoS Pathog.* **2020**;16(11):e1009010. doi:[10.1371/journal.ppat.1009010](https://doi.org/10.1371/journal.ppat.1009010).
15. Velasquez DE, Parashar U, Jiang B. Decreased performance of live attenuated, oral rotavirus vaccines in low-income settings: causes and contributing factors. *Expert Rev Vaccines.* **2018**;17:1–17. doi:[10.1080/14760584.2018.1418665](https://doi.org/10.1080/14760584.2018.1418665).
16. Mwila K, Chilengi R, Simuyandi M, Permar SR, Becker-Dreps S. Contribution of maternal immunity to decreased rotavirus vaccine performance in low- and middle-income countries. *Clin Vaccine Immunol.* **2017**;24(1). doi:[10.1128/CVI.00405-16](https://doi.org/10.1128/CVI.00405-16).
17. Desselberger U. Differences of rotavirus vaccine effectiveness by country: likely causes and contributing factors. *Pathogens.* **2017**;6(4):6. doi:[10.3390/pathogens6040065](https://doi.org/10.3390/pathogens6040065).
18. Rogawski ET, Platts-Mills JA, Colgate ER, Haque R, Zaman K, Petri WA, Kirkpatrick BD. Quantifying the impact of natural immunity on rotavirus vaccine efficacy estimates: a clinical trial in Dhaka, Bangladesh (PROVIDE) and a simulation study. *J Infect Dis.* **2018**;217(6):861–68. doi:[10.1093/infdis/jix668](https://doi.org/10.1093/infdis/jix668).
19. Parker EP, Ramani S, Lopman BA, Church JA, Iturriza-Gomara M, Prendergast AJ, Grassly NC. Causes of impaired oral vaccine efficacy in developing countries. *Future Microbiol.* **2018**;13(1):97–118. doi:[10.2217/fmb-2017-0128](https://doi.org/10.2217/fmb-2017-0128).
20. Resch TK, Wang Y, Moon SS, Joyce J, Li S, Prausnitz M, Jiang B. Inactivated rotavirus vaccine by parenteral administration induces mucosal immunity in mice. *Sci Rep.* **2018**;8(1):561. doi:[10.1038/s41598-017-18973-9](https://doi.org/10.1038/s41598-017-18973-9).
21. Wang Y, Zade J, Moon SS, Weldon W, Pisal SS, Glass RI, Dhere RM, Jiang B. Lack of immune interference between inactivated polio vaccine and inactivated rotavirus vaccine co-administered by intramuscular injection in two animal species. *Vaccine.* **2019**;37(5):698–704. doi:[10.1016/j.vaccine.2018.12.043](https://doi.org/10.1016/j.vaccine.2018.12.043).
22. Yin N, Wu J, Kuang X, Lin X, Zhou Y, Yi S, Hu X, Chen R, Liu Y, Ye J, et al. Vaccination of pregnant rhesus monkeys with inactivated rotavirus as a model for achieving protection from rotavirus SA11 infection in the offspring. *Hum Vaccin Immunother.* **2021**;17(12):5656–65. doi:[10.1080/21645515.2021.2011548](https://doi.org/10.1080/21645515.2021.2011548).
23. Lakatos K, McAdams D, White JA, Chen D. Formulation and preclinical studies with a trivalent rotavirus P2-VP8 subunit vaccine. *Hum Vaccin Immunother.* **2020**;16:1957–68. doi:[10.1080/21645515.2019.1710412](https://doi.org/10.1080/21645515.2019.1710412).
24. Groome MJ, Koen A, Fix A, Page N, Jose L, Madhi SA, McNeal M, Dally L, Cho I, Power M, et al. Safety and immunogenicity of a parenteral P2-VP8-P[8] subunit rotavirus vaccine in toddlers and infants in South Africa: a randomised, double-blind, placebo-controlled trial. *Lancet Infect Dis.* **2017**;17(8):843–53. doi:[10.1016/S1473-3099\(17\)30242-6](https://doi.org/10.1016/S1473-3099(17)30242-6).
25. Groome MJ, Fairlie L, Morrison J, Fix A, Koen A, Masenya M, Jose L, Madhi SA, Page N, McNeal M, et al. Safety and immunogenicity of a parenteral trivalent P2-VP8 subunit rotavirus vaccine: a multisite, randomised, double-blind, placebo-controlled trial. *Lancet Infect Dis.* **2020**;20(7):851–63. doi:[10.1016/S1473-3099\(20\)30001-3](https://doi.org/10.1016/S1473-3099(20)30001-3).
26. Wang Y, Azevedo M, Saif LJ, Gentsch JR, Glass RI, Jiang B. Inactivated rotavirus vaccine induces protective immunity in gnotobiotic piglets. *Vaccine.* **2010**;28(33):5432–36. doi:[10.1016/j.vaccine.2010.06.006](https://doi.org/10.1016/j.vaccine.2010.06.006).
27. Velasquez DE, Wang Y, Jiang B. Inactivated human rotavirus vaccine induces heterotypic antibody response: correction and development of IgG avidity assay. *Hum Vaccin Immunother.* **2015**;11(2):531–33. doi:[10.4161/21645515.2014.988553](https://doi.org/10.4161/21645515.2014.988553).
28. Jiang B, Estes MK, Barone C, Barniak V, O’neal CM, Otaiano A, Madore HP, Conner ME. Heterotypic protection from rotavirus infection in mice vaccinated with virus-like particles. *Vaccine.* **1999**;17(7–8):1005–13. doi:[10.1016/S0264-410X\(98\)00317-X](https://doi.org/10.1016/S0264-410X(98)00317-X).
29. Jiang B, Wang Y, Glass RI. Does a monovalent inactivated human rotavirus vaccine induce heterotypic immunity? Evidence from animal studies. *Hum Vaccin Immunother.* **2013**;9(8):1634–37. doi:[10.4161/hv.24958](https://doi.org/10.4161/hv.24958).
30. Fix AD, Harro C, McNeal M, Dally L, Flores J, Robertson G, Boslego JW, Cryz S. Safety and immunogenicity of a parenterally administered rotavirus VP8 subunit vaccine in healthy adults. *Vaccine.* **2015**;33(31):3766–72. doi:[10.1016/j.vaccine.2015.05.024](https://doi.org/10.1016/j.vaccine.2015.05.024).
31. Zhang B, Yi S, Ma Y, Zhang G, Zhang Y, Xie T, Li H, Sun M. Immunogenicity of a scalable inactivated rotavirus vaccine in mice. *Hum Vaccin.* **2011**;7(2):248–57. doi:[10.4161/hv.7.2.14121](https://doi.org/10.4161/hv.7.2.14121).
32. Wu JY, Zhou Y, Zhang GM, Mu GF, Yi S, Yin N, Xie Y-P, Lin X-C, Li H-J, Sun M-S. Isolation and characterization of a new candidate human inactivated rotavirus vaccine strain from hospitalized children in Yunnan, China: 2010–2013. *World J Clin Cases.* **2018**;6(11):426–40. doi:[10.12998/wjcc.v6.i11.426](https://doi.org/10.12998/wjcc.v6.i11.426).
33. Zhou Y, Hu X, Chen R, Wu J, Lin X, Lu C, Yin N, Tang Y, Shi P, Song Z, et al. Impact of maternal and pre-existing antibodies on immunogenicity of inactivated rotavirus vaccines. *Vaccine.* **2022**;40(28):3843–50. doi:[10.1016/j.vaccine.2022.05.036](https://doi.org/10.1016/j.vaccine.2022.05.036).
34. Berkopac A. HyperQuick algorithm for discrete hypergeometric distribution. *J Discrete Algorithms.* **2007**;5(2):341. doi:[10.1016/j.jda.2006.01.001](https://doi.org/10.1016/j.jda.2006.01.001).

35. Franz M, Rodriguez H, Lopes C, Zuberi K, Montojo J, Bader GD, Morris Q. GeneMANIA update 2018. *Nucleic Acids Res.* **2018**;46(W1):W60–4. doi:[10.1093/nar/gky311](https://doi.org/10.1093/nar/gky311).
36. Montojo J, Zuberi K, Rodriguez H, Bader GD, Morris Q. GeneMANIA: fast gene network construction and function prediction for cytoscape. *F1000research.* **2014**;3:153. doi:[10.12688/f1000research.4572.1](https://doi.org/10.12688/f1000research.4572.1).
37. Jalilvand S, Marashi SM, Shoja Z. Rotavirus VP6 preparations as a non-replicating vaccine candidates. *Vaccine.* **2015**;33(29):3281–87. doi:[10.1016/j.vaccine.2015.05.026](https://doi.org/10.1016/j.vaccine.2015.05.026).
38. Gandhi GR, Santos VS, Denadai M, da Silva Calisto VK, de Souza Siqueira Quintans J, de Oliveira ESAM, de Souza Araújo AA, Narain N, Cuevas LE, Júnior LJQ, et al. Cytokines in the management of rotavirus infection: a systematic review of in vivo studies. *Cytokine.* **2017**;96:152–60. doi:[10.1016/j.cyto.2017.04.013](https://doi.org/10.1016/j.cyto.2017.04.013).
39. Ye L, Jiang Y, Yang G, Yang W, Hu J, Cui Y, Shi C, Liu J, Wang C. Murine bone marrow-derived DCs activated by porcine rotavirus stimulate the Th1 subtype response in vitro. *Microb Pathog.* **2017**;110:325–34. doi:[10.1016/j.micpath.2017.07.015](https://doi.org/10.1016/j.micpath.2017.07.015).
40. Mahmoudzadeh S, Nozad Charoudeh H, Marques CS, Bahadory S, Ahmadpour E. The role of IL-12 in stimulating NK cells against Toxoplasma gondii infection: a mini-review. *Parasitol Res.* **2021**;120(7):2303–09. doi:[10.1007/s00436-021-07204-w](https://doi.org/10.1007/s00436-021-07204-w).
41. Tait Wojno ED, Hunter CA, Stumhofer JS. The immunobiology of the interleukin-12 family: room for discovery. *Immunity.* **2019**;50(4):851–70. doi:[10.1016/j.immuni.2019.03.011](https://doi.org/10.1016/j.immuni.2019.03.011).
42. Holmgren J, Parashar UD, Plotkin S, Louis J, Ng SP, Desauzier E, Picot V, Saadatian-Elahi M. Correlates of protection for enteric vaccines. *Vaccine.* **2017**;35(26):3355–63. doi:[10.1016/j.vaccine.2017.05.005](https://doi.org/10.1016/j.vaccine.2017.05.005).
43. Desselberger U, Huppertz HI. Immune responses to rotavirus infection and vaccination and associated correlates of protection. *J Infect Dis.* **2011**;203(2):188–95. doi:[10.1093/infdis/jiq031](https://doi.org/10.1093/infdis/jiq031).
44. Angel J, Steele AD, Franco MA. Correlates of protection for rotavirus vaccines: possible alternative trial endpoints, opportunities, and challenges. *Hum Vaccin Immunother.* **2014**;10(12):3659–71. doi:[10.4161/hv.34361](https://doi.org/10.4161/hv.34361).
45. Clarke E, Desselberger U. Correlates of protection against human rotavirus disease and the factors influencing protection in low-income settings. *Mucosal Immunol.* **2015**;8(1):1–17. doi:[10.1038/mi.2014.114](https://doi.org/10.1038/mi.2014.114).
46. Caddy SL, Vaysburd M, Wing M, Foss S, Andersen JT, O'Connell K, Mayes K, Higginson K, Ituriza-Gómez M, Desselberger U, et al. Intracellular neutralisation of rotavirus by VP6-specific IgG. *PLoS Pathog.* **2020**;16(8):e1008732. doi:[10.1371/journal.ppat.1008732](https://doi.org/10.1371/journal.ppat.1008732).
47. Campbell JS, Davidson AJ, Todd H, Rodrigues F, Elliot AM, Early JJ, Lyons DA, Feng Y, Wood W. PTPN21/Pez is a novel and evolutionarily conserved key regulator of inflammation in vivo. *Curr Biol.* **2021**;31(4):875–83 e5. doi:[10.1016/j.cub.2020.11.014](https://doi.org/10.1016/j.cub.2020.11.014).
48. Zhu L, Yin H, Qian T, Qi GJ, Ren JS, Wang Y, Qi B-X. Distinct expression and clinical value of aquaporin 4 in children with hand, foot and mouth disease caused by enterovirus 71. *J Med Virol.* **2022**;94(2):587–93. doi:[10.1002/jmv.25475](https://doi.org/10.1002/jmv.25475).
49. Zhao Y, Howatt DA, Gizard F, Nomiyama T, Findeisen HM, Heywood EB, Jones KL, Conneely OM, Daugherty A, Bruemmer D. Deficiency of the NR4A orphan nuclear receptor NOR1 decreases monocyte adhesion and atherosclerosis. *Circ Res.* **2010**;107(4):501–11. doi:[10.1161/CIRCRESAHA.110.222083](https://doi.org/10.1161/CIRCRESAHA.110.222083).
50. Ostermann G, Weber KS, Zernecke A, Schroder A, Weber C. JAM-1 is a ligand of the β2 integrin LFA-1 involved in transendothelial migration of leukocytes. *Nat Immunol.* **2002**;3(2):151–58. doi:[10.1038/ni755](https://doi.org/10.1038/ni755).
51. Fraemohs L, Koenen RR, Ostermann G, Heinemann B, Weber C. The functional interaction of the β2 integrin lymphocyte function-associated antigen-1 with junctional adhesion molecule-A is mediated by the I domain. *J Immunol.* **2004**;173(10):6259–64. doi:[10.4049/jimmunol.173.10.6259](https://doi.org/10.4049/jimmunol.173.10.6259).
52. Korbecki J, Barczak K, Gutowska I, Chlubek D, Baranowska-Bosiacka I. CXCL1: gene, promoter, regulation of expression, mRNA stability, regulation of activity in the intercellular space. *Int J Mol Sci.* **2022**;23(2):792. doi:[10.3390/ijms23020792](https://doi.org/10.3390/ijms23020792).
53. Singh A, Bisht P, Bhattacharya S, Guchhait P. Role of platelet cytokines in dengue virus infection. *Front Cell Infect Microbiol.* **2020**;10:561366. doi:[10.3389/fcimb.2020.561366](https://doi.org/10.3389/fcimb.2020.561366).
54. Karin N, Wildbaum G. The role of chemokines in adjusting the balance between CD4+ effector T cell subsets and FOXP3-negative regulatory T cells. *Int Immunopharmacol.* **2015**;28(2):829–35. doi:[10.1016/j.intimp.2015.03.037](https://doi.org/10.1016/j.intimp.2015.03.037).